Facile Formation of Ordered Vertical Arrays by Droplet Evaporation of Au Nanorod Organic Solutions

Alfonso Martín, Carola Schopf*, Andrea Pescaglini*, Jin Jin Wang†, Daniela Iacopino***

*Tyndall National Institute, Dyke Parade, Cork, Ireland

† Centre for Research on Adaptive Nanostructures and Nanodevices (CRANN), Trinity College Dublin, College Green, Dublin, Ireland.

KEYWORDS Au nanords, vertical arrays, self-assembly, droplet deposition, SERS.

ABSTRACT

Droplet evaporation is a simple method to induce organization of Au nanorods into ordered superstructures. In general, the self-assembly process occurs by evaporation of aqueous suspensions under strictly controlled experimental conditions. Here we present formation of large area ordered vertical arrays by droplet evaporation of Au nanorod organic suspensions. The uncontrolled (free air) evaporation of such suspensions yielded to formation of ordered nanorod domains covering the entire area of a 5 mm diameter droplet. Detailed investigation of the process revealed that nanorods organized into highly ordered vertical domains at the interface between solvent and air on a fast time scale (minutes). The self-assembly process mainly

depended on the initial concentration of nanorod solution and required minimal control of other experimental parameters. Nanorod arrays displayed distinct optical properties which were analyzed by optical imaging and spectroscopy and compared to results obtained from theoretical calculations. The potential use of synthesized arrays as surface-enhanced Raman scattering probes was demonstrated with model molecule 4-aminobenzenthiol.

Introduction

The elongated shape of Au nanorods and their consequent intriguing optical properties are highly attractive for catalytic, plasmonic and biomedical applications.[1] The controllable assembly of Au nanorods into large-scale ordered superstructures is also attractive, as it can generate additional intriguing properties arising from the collective inter-particle coupling of the assembled components.[2] Among possible assembly geometries, the 2-dimensional (2D) hexagonal sheet (honeycomb) structure that is formed from vertically oriented nanorods is regarded as the ideal configuration for many technological devices (ie. solar cells and memory devices).[3] Moreover, applications such as surface-enhanced Raman scattering (SERS), cavity resonators, nanoscale light polarizers and ultrafast non-linear optics have been envisaged for vertically aligned Au nanorod superstructures.[4-6]

Common approaches used for fabrication of Au nanorod vertical arrays on substrates include template-mediated methodologies,[7] oblique angle deposition[8-9] and self-assembly on patterned substrates.[10-11] Recently, droplet evaporation has been proposed as simple and relatively fast method for formation of large area nanorod superstructures.[12] The process consists into depositing a droplet of nanorod solution (usually water) on a substrate (usually silicon) and let the solvent evaporate under controlled conditions. The assembly is driven by relatively weak attractive forces (van der Waals, dipole-dipole interactions), becoming relevant as the solvent

evaporates. Also electrostatic repulsive forces, hydrophobic interactions, capillary forces and entropic depletion interactions play a role that mediate nanostructure's self-assembly.

The evaporation mediated process is affected by several parameters (such as nanorod concentration, surfactant, evaporation rate, nanorod aspect ratio and substrate, among others), which have to be controlled in order to obtain the desired assembly geometry. For example Liz-Marzán *et al*. used cationic Gemini surfactants for the growth of Au nanorods which self-assembled into highly ordered, multilayer vertical arrays.[13,14] In a similar manner, the modification of nanorod surfaces by glycol/thiols induced formation of ordered vertical arrays.[15] Also, Xiong *et al.* fabricated closely spaced vertical nanorod arrays by altering the ionic strength of the deposited nanorod solution[16] whereas Xie et al used two stages controlled evaporation methods to obtain large area ordered vertical arrays.[17] Thus, the simplicity and flexibility of the method makes droplet evaporation processes highly suitable for fabrication of nanorod ordered arrays. However, the ability to induce high degree of order in the self-assembly process is still limited by the necessary use of appropriate, often long, drying conditions and warrants careful control of several parameters. Moreover, the use of droplet evaporation techniques for fabrication of structures with a high degree of order that extends over large areas has, to date, proven challenging.

In contrast to the vast literature dedicated to theoretical and experimental investigation of the mechanisms regulating the droplet evaporation-induced self-assembly in Au nanorods from aqueous suspensions, limited attention has been dedicated to self-assembly processes occurring into evaporating nanostructure organic suspensions.[18,19] Nevertheless, the ability to induce large area order into such suspensions would extend applications of metal nanostructures, potentially leading to development of hybrid devices with enhanced optoelectronic properties.

Recently, our group has explored the self-assembly properties of Au nanorods dispersed in organic solvents. Droplet evaporation of Au nanorod (11×41 nm) chlorobenzene solutions under controlled conditions (slow evaporation, ca. 3 h) yielded to formation of nematic superstructures where nanorods assembled parallel to a substrate in extended side-by-side configurations.[21] Fabricated superstructures displayed enhanced plasmon induced photoconductance sensitive to the linear polarization of the exciting photons at wavelengths corresponding to the excitation of the nanorods longitudinal surface plasmon resonance.[22]

In this work, we present a facile and fast approach for fabrication of large area vertical nanorod arrays by droplet evaporation of Au nanorod organic suspensions. Nanorods (23 × 54 nm) were synthesized in water and subsequently phase-transferred into chlorobenzene. The simple evaporation of a nanorod chlorobenzene droplet under uncontrolled conditions (free air, 20 min) lead to formation of vertical nanorod monolayer superstructures covering the entire area of the deposited droplet (20 mm^2). The assembly process was found to be prevalently dependent on nanorod concentration, whereas the influence of other parameters was negligible. At low concentrations nanorods assembled vertically into domains, with the area between domains occupied by nanorods deposited horizontally to the substrate. At high concentrations density and size of domains increased until the entire area of the droplet was covered by vertical superstructures. Observation of droplet evaporation process under microscope light revealed that nanorods assembled at the interface between solvent and air, forming domains that grew in size and density as the solvent evaporated. The optical properties of obtained superstructures were characterized both theoretically and experimentally. Finally, the potential use of fabricated arrays for analytical detection based on SERS was demonstrated using 4-aminobenzethiol as model analyte.

Materials and Methods

Materials. Tetrachloroauric acid, silver nitrate, sodium borohydride, ascorbic acid, hydrochloric acid, chlorobenzene, cetyltrimethylammoniumbromide (CTAB), mercaptosuccinic acid, tetraoctylammoniumbromide (TOAB), 4-aminobenzethiol (4-ABT) were purchased from Sigma-Aldrich. All glassware was cleaned with acqua regia prior to nanorod synthesis. Milli-Q water (resistivity > 18 MΩ cm-1) was used throughout the experiments.

Synthesis of Au nanorods. Au nanorods (AR = 2.3) were synthesized by overgrowth of seed-mediated method reported by Liz-Marzán *et al.*[23] As-prepared Au nanorods were centrifuged and redispersed into water, in order to maintain a CTAB concentration between 0.1 mM and 0.35 mM. Au nanorods in water solutions were transferred in chlorobenzene following the method described by Chen.[24] In particular, Au nanorods in water solution were centrifuged and redispersed in water so that the final CTAB concentration was lower than 0.2 mM. Mercapto-succinic acid (3 mL, 10 mM) was added to 3 mL of aqueous nanorod solution. The pH was adjusted to 9 under vigorous stirring. To this solution 1.5 mL of a 50 mM solution of TOAB in chlorobenzene was added. The resulting mixture was left under vigorous stirring for 30 min until the water phase discolored and the organic phase became intense red. Details of synthesis and spectral characteristics of aqueous and organic phase nanorods are reported in the SI.

Fabrication of ordered Au nanorod superstructures. A small aliquot (10 μL) of Au nanorod cholobenzene solution ([Au] = 1.4 nM -14 nM) was deposited on SiO_2 or glass substrate and left to evaporate under free air over ca. 20 min.

Scanning electron microscopy (SEM) images of nanorod solutions and nanorod Fast Fourier Transforms (FFT) were acquired using a field emission SEM (JSM-6700F, JEOL UK Ltd.) operating at beam voltages of 2 kV.

Optical Characterisation. White light (reflection) optical images of vertical arrays were acquired using an Axioscop II microscope (Carl Zeiss, Inc.) equipped with a 100 W halogen lamp. Transmission spectra of gold nanorod arrays were acquired with an inverted IX-71 Olympus microscope with a 100X objective. The sample was illuminated with a 100 W halogen lamp. The light collected by the objective was directed into the entrance of slit of a monochromator (SP-300i, Acton Research) equipped with a thermoelectrically cooled, back illuminated CCD (Spec10:100B, Princeton Instruments) for spectra acquisition. The sample polarization rate was determined by a polarizer placed between the lamp and the sample. Spectra were typically recorded using an integration time of 1-10 s. The extinction was calculated according to Lambert-Beer's law: $A= -\log10(I/I_0)$ with I being the sample spectrum and I_0 being the blank spectrum taken from a nearby clean area on the substrate.

Raman spectra were obtained from a Renishaw inViaRaman system. A 632.8nm helium-neon laser was employed as an excitation source. The laser beam was focused onto the sample through a Mitutoyo M Plan Apo 100X objective with 0.7 N.A. Measured power at the sampling level was controlled at about 5mW. Acquisition time was usually 10 s. To obtain SERS spectra, 5 μL of 4-ABT (chlorobenzene, 1 mM) were mixed with 5 μL of Au nanorod solution (Chlorobenzene, 14 nM) and left to evaporate over 20 min.

Theoretical Simulations. Extinction spectra where simulated by solving the Maxwell's equations using a boundary element method with MNPBEM Matlab toolbox. A 6×6 vertical array of nanorods of dimensions 20×60 nm was considered.

Results and discussions

Au nanorods were synthesized by a combined seed-mediated/overgrowth method described by Liz-Marzán *et al.*[23] Nanorods of average size 14 ± 2 nm × 44 ± 3 nm were firstly synthesized by seed mediated method and subsequently overgrown to a final mean size of 23 ± 3 nm × 54 ± 3 nm, aspect ratio (AR) = 2.3, by further addition of reducing agent ascorbic acid. The as prepared Au nanorod solution (10 mL) was centrifuged twice to remove cetyltrimetylammonium bromide (CTAB) excess and re-dispersed in 10 mL of Millipore water. The final CTAB concentration was kept between 0.1 mM and 0.35 mM. Prior to deposition on solid substrates, nanorods were transferred into chlorobenzene following the method described by Chen *et al.*[24] It should be pointed out that only nanorods synthesized by the overgrowth method formed ordered vertical arrays upon transfer into organic phase. In comparison, droplet evaporation of equivalent size nanorod chlorobenzene suspensions obtained by simple seed mediated method produced ordered superstructures constituted by nanorods aligned horizontal to a substrate in a side-by-side fashion.[20-21,25]

Ordered arrays were obtained by deposition of Au nanorod chlorobenzene solutions onto an arbitrary substrate, followed by evaporation of the droplet under free air over 20 min. Figure 1a shows a low magnification SEM image of a dried droplet deposited onto a SiO_2 substrate showing uniform coverage of the entire 20 mm^2 droplet. Closer observation (Figure 1b) revealed that nanords assembled into closely spaced domains of average size 2 μm^2, which covered ca. 90% of the droplet surface, as estimated from statistical analysis performed on SEM images by image J program. The interstices between adjacent domains were filled by nanorods lying horizontal to the substrate. High

SEM magnification image of an individual domain (Figure 1c) showed formation of a 2D solid and highly ordered phase where nanorods aligned with their long axes perpendicular to the substrate. The nanorods were organized into closely packed ordered hexagonal structures, as revealed by the fast Fourier transform analysis showed as inset in Figure 1c. Evidence of monolayer formation is shown in Figure 1d, depicting the edge of an isolated nanorod domain.

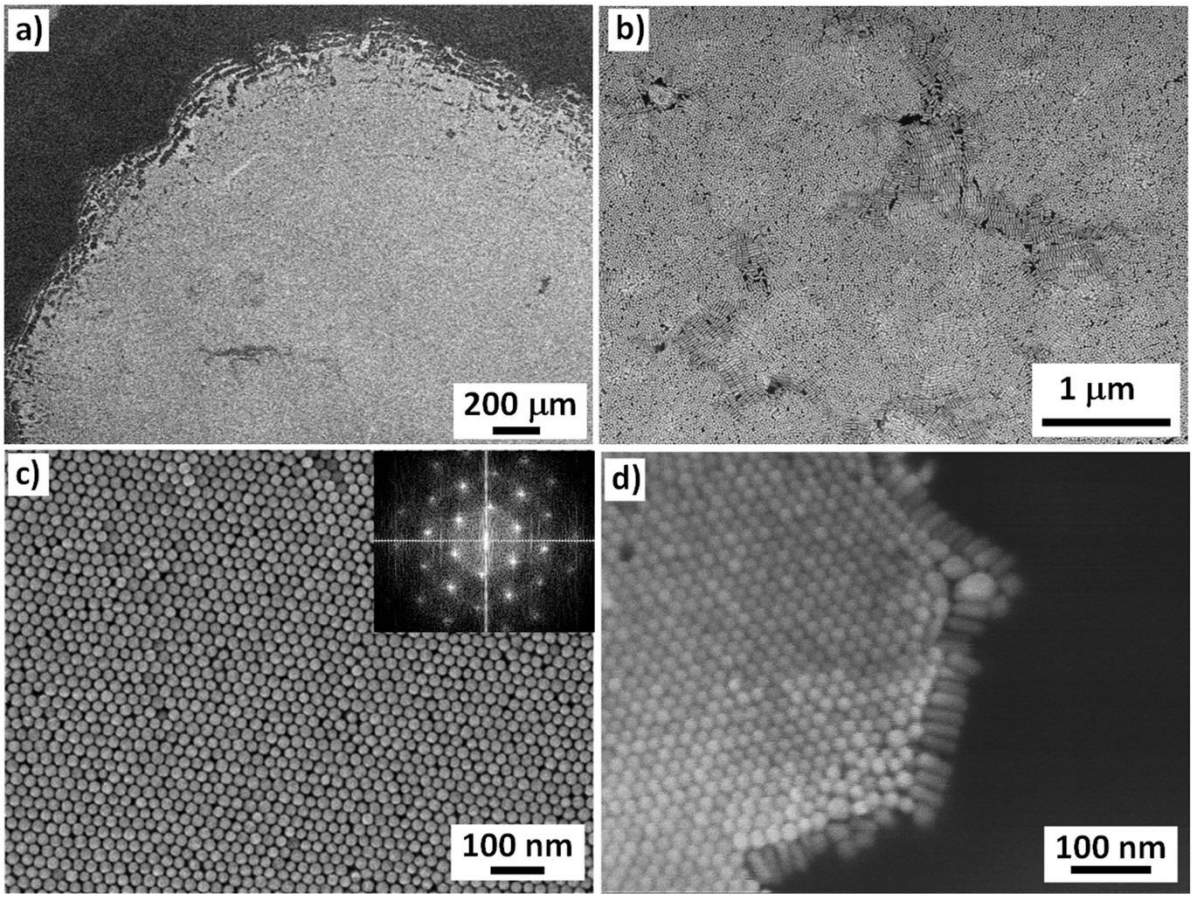

Figure 1. SEM images of Au nanorod vertical arrays obtained by droplet evaporation of nanorod chlorobenzene solutions on SiO_2; a) low magnification image of dried deposited droplet; b) low magnification image showing assembly of nanorods into closely-spaced domains; c) high magnification image showing vertical alignment of Au nanorods within an individual domain.

Inset: Fast Fourier Transform of the image shown in c); d) image of a nanorod domain showing evidence of monolayer formation.

In order to gain a deeper understanding of the mechanism regulating the formation of Au superstructures during droplet evaporation, investigation of the effects played by the following parameters was undertaken: nanorod solution concentration, surfactant, substrate, nanorod aspect ratio, evaporation rate and solvent.

Ordered assemblies formed across a relatively large range of Au nanorod concentrations, between 1.4 nM and 14 nM. The increase in concentration affected the size of the deposited dried droplet, which varied from 1.5 mm in diameter to 5 mm in diameter, respectively. This effect is shown in the photographs of the droplet reported in Figure 2a. For all droplets the initial deposited solution was 10 μL. The final size of the dried droplet was determined by the evaporation of chlorobenzene, during which assembled domains were brought close to each other and assembled into compact arrays at the last stages of droplet evaporation (see Figure 4 for more details).

Domain size, density and compactness were also found to be dependent on the initial nanorod solution concentration. Figure 2b reports the vertical array surface coverage estimated for deposited nanorod solution concentrations 1.4 nM, 3 nM, 6 nM and 14 nM with CTAB concentration of 0.1 mM and 0.35 mM, respectively. The surface coverage was calculated using optical images (Figure S4, S5) and was defined as the ratio between the area occupied by the vertical arrays and the total area of the optical image. At low concentrations nanorods arranged vertically into distinct domains of 2 μm^2 average size (see also SEM images in Figure S3), which covered an area corresponding to 34% of the total area occupied by the droplet. The remaining 66% of the droplet was constituted by

empty spaces and areas where nanorods deposited with their long axes horizontal to the substrate. As nanorod concentration increased (3 mM) domain density increased to 64%. Also, for nanorod concentrations of 6 nM and higher, domains grew to an average size of 20 μm^2, and individual domains merged covering the entire area of the droplet (estimated coverage area 94%). The progressive increase of surface coverage for three representative Au nanorod concentrations is captured on the optical images shown in Figure 2b as insets.

Figure 2b also reports the effect of CTAB concentration for increasing Au nanorod solution concentrations. The percentage of surface coverage at higher CTAB concentrations (0.35 mM) increased from 34% to 57% as nanorod concentration increased from 1.4 nM to 14 nM, thus remaining lower than the corresponding increase from 34% to 94% observed for [CTAB] = 0.1 mM. The concentration of CTAB is known to play an important role on the self-assembly process of Au nanorods with reports in literature that higher CTAB concentrations are favorable to formation of more stable assemblies.[15] In contrast, our data show that the best quality of assemblies (in terms of surface coverage and ratio between vertical nanorod domains and deposited horizontal nanorods) formed when the CTAB concentration was kept closer to the low value of 0.1 mM. The fact that nanorods could not be successfully transferred into organic phase at CTAB concentrations lower than 0.1 mM or higher than 0.35 mM, prevented the exploration of larger concentration ranges. Variation of tetraoctylammoniumbromide (TOAB) concentration from the 50 mM value used for phase transfer did not affect the final degree of order obtained. However, the concentration of TOAB affected the stability of nanorod chlorobenzene suspensions which were stable for over two weeks

with [TOAB] = 50 mM and for less than a week at lower (25 mM and below) TOAB concentrations.

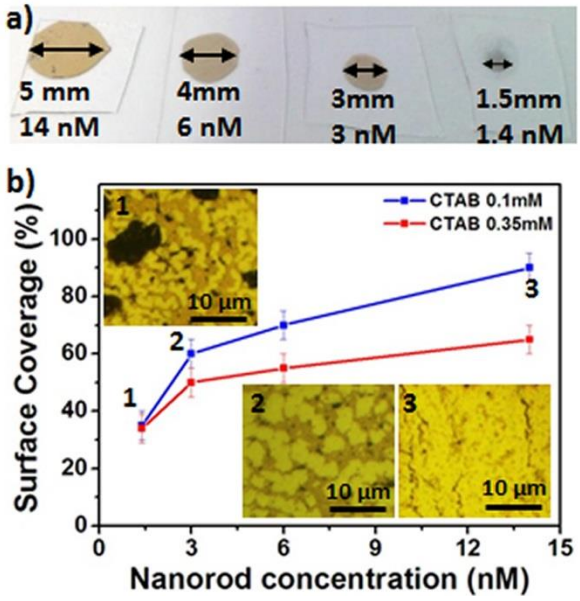

Figure 2. a) photographs of dried droplets obtained from Au nanorods chlorobenzene solutions of decreasing concentrations (14 nM to 1.4 nM. Diameter of deposited droplet was 7 mm; b) Surface coverage *vs* nanorod concentration for CTAB concentrations 0.35 nM and 0.1 nM and Au nanorods chlorobenzene solutions of increasing concentrations (1.4 to 14 nM). Insets: representative optical reflection images of coverages obtained under conditions of points 1-3.

Regarding the effect of substrates, vertical superstructures of comparable high order were obtained from droplet evaporation on SiO_2, glass and glass/ITO substrates (measured contact angles 52°, 40º and 72° respectively). Also, the nanorod dimension did not affect the assembly process, which produced equally ordered vertical arrays with nanorods of slightly different aspect ratios (from 2.3 to 3.1, Figure S6).

In order to investigate the effect of the evaporation rate the deposited droplet was covered with a petri dish in order to slow the evaporation rate to ca. 3 h. Nanorods self-assembled into compact and well ordered vertical arrays (see Figure S7) on the periphery of the droplet, in an area corresponding to ca. 25% of the entire droplet area. This process is displayed in Figure 3a showing a low magnification SEM image of a dried droplet obtained by slow evaporation of a nanorod solution 6 nM. As can be easily seen, nanorods assembled vertically at the periphery of the ring, within the marked area (see top right inset of Figure 3a). Outside the marked area nanorods mainly aligned side-to-side horizontal to the substrate were found to partially cover the surface, as shown in the bottom left inset of Figure 3a. The vertical array surface coverage achieved with the slow evaporation method for nanorods of different concentrations ([CTAB] = 0.1 mM) is summarized in Figure 3b. At the periphery of the droplet coverage increased slightly from 78% at [Au nanorod] = 1.4 nM to 83% at [Au nanorod] = 14 nM (black continuous line). In the center of the droplet the area occupied by vertical arrays grew from 16% to 81% for [Au nanorod] = 1.4 nM and 14 nM, respectively (black, dashed line). For comparison, the coverage calculated for free air assembly is also reported in Figure 3b as green line. Our findings were in agreement with results obtained by Xie *et al.* who obtained self-assembled vertical arrays at the periphery of a droplet by using a two stages (slow followed by fast evaporation) droplet evaporation method.[17]

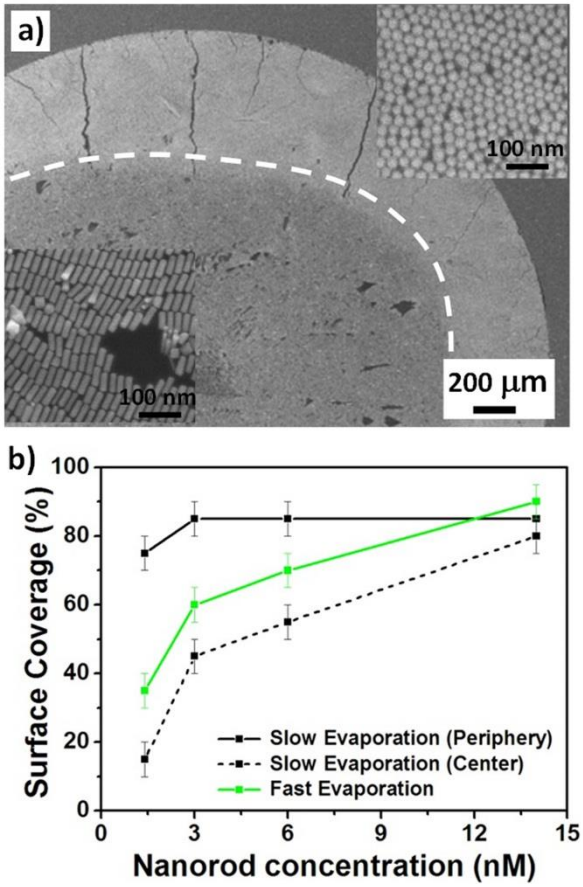

Figure 3. a) SEM image of assembly obtained from slow evaporation of nanorod chlorobenzene solutions ([Au] = 6 nM). Insets: representative SEM images of assemblies obtained at the periphery (top right) and center (bottom left) of the droplet; b) surface coverage of vertical arrays obtained under slow evaporation at both the periphery (black continuous curve) and the center (black dashed curve) of the droplet. Green curve show the comparison with coverages obtained by fast (free air) evaporation.

Finally, the use of the chlorobenzene solvent was essential for the generation of long-range ordering observed in our superstructures. Analogous droplet deposition of Au nanorod aqueous solutions (14 nM, Figure S7) produced accumulation of nanorods into the periphery of the droplet with formation of dense multilayer vertical and parallel

arrays. Sparse mixed parallel and vertical assemblies were found in the center of the droplet, in agreement with coffee-stain mechanisms. The high degree of order obtained from chlorobenzene dispersions was attributed to the lower surface tension and lower viscosity of chlorobenzene compared to water. These factors promoted a higher degree of ordering by offering less resistance to domain movement, thus allowing more nanorods to be at an equilibrium position and assemble together in the solution before droplet evaporation.

Observation of the evaporation process under optical microscope revealed that nanorods organized into vertically aligned domains at the interface between solvent and air. Photographs of evaporation stages for a droplet deposited on a glass surface (Figure 4a-d) display color transition from red to gold associated to the progressive organization of nanorods into arrays. Figure 4e-g show optical reflection images of an evaporating droplet, highlighting formation and growth of nanorod domains. We ascribed the assembly of nanorods into vertical superstructures to a balance between repulsive electrostatic and steric forces and van der Waals attractive hydrophobic interactions between the CTAB/TOAB alkyl chains deposited on the surface of Au nanorods. Also, attractive micelles forces coming into play when the concentration of surfactant increased due to solvent evaporation probably contributed to stabilize the rods within an effective separation. After formation of initial domains, assemblies continued to grow with the incoming nanorods until solvent completely evaporated. The high electrostatic repulsion between the domains in solution was the most probable cause of monolayer formation. The intense colors displayed under polarized transmission illumination (Figure 4h)

suggest that formed superstructures possess intriguing collective plasmon modes that could be excited by polarized light.[20,26]

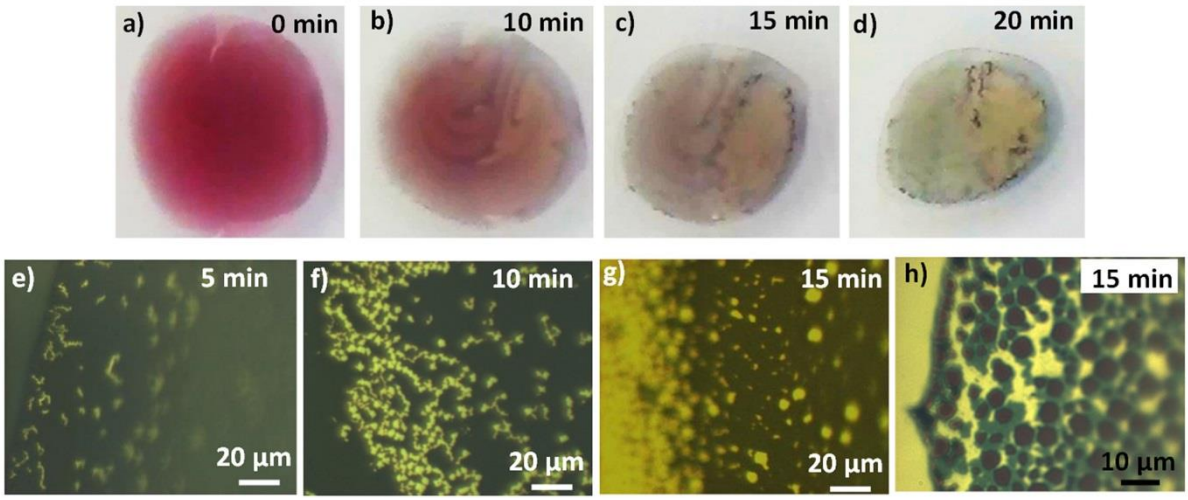

Figure 4. a-b) Photographs of drying stages of a Au nanorod droplet deposited on glass coverslip; e-g) optical reflection images of drying droplet showing progressive formation and growth of nanorod domains; h) optical polarized transmission image of drying droplet.

The investigation of self-assembled structure optical properties is critical to unlock potential applications requiring control and tunability of superstructure's optical properties. Towards this end, we measured extinction spectra of nanorod vertical arrays and compared experimental data with theoretical data obtained by solving the Maxwell's equations using a boundary element method with MNPBEM Matlab toolbox. Figure 5a reports experimental extinction spectrum of vertical superstructures. The spectrum was characterized by one broad peak centered at 660 nm, in contrast with the spectrum of nanorods in solution reported as inset in Figure 5a, showing two distinct peaks at 520 and 660 nm related to the transversal and longitudinal plasmon modes, respectively. The simulated extinction spectrum of a 6×6 nanorod array with inter-nanorod spacing of 1.2 nm is shown in Figure 5b. The light

propagation direction was along the z axis and light was polarized along the x direction (see inset). The extinction spectrum was characterized by a broad peak at 620 nm, in reasonable agreement with the experimental data (considering the small size of the simulated array compared to the size of the measured array). Simulated absorption and scattering spectra are also shown in Figure 3b, showing maxima centered at 600 and 626 nm, respectively. It should be pointed out that vertical assemblies could not be obtained on TEM grids, therefore an exact estimation of the internanorod distance has not been possible. However, various groups have reported inter-nanorod distances smaller than 2 nm, as result of strong inter-digitation of CTAB molecules occurring during the assembly process.[27-28]

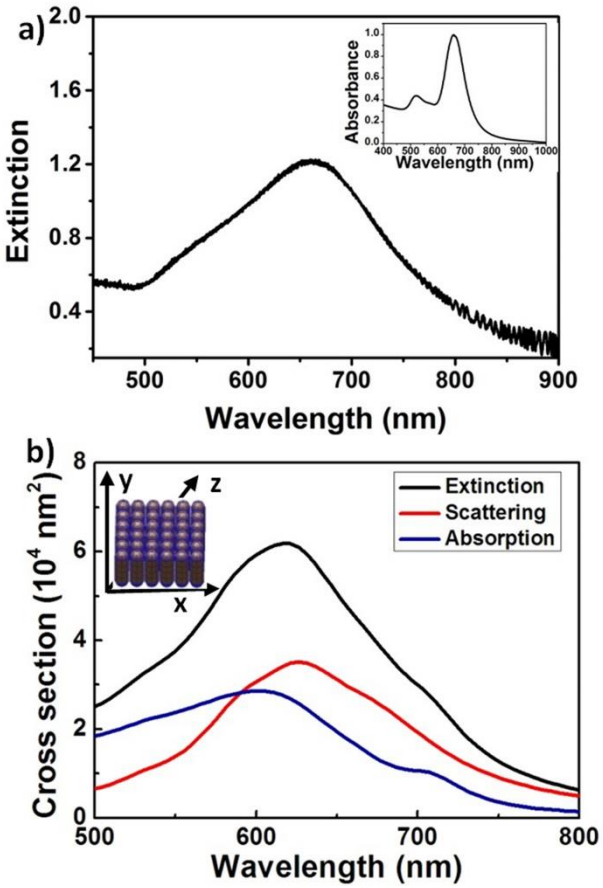

Figure 5. a) Extinction spectrum of nanorods arranged into perpendicular arrays measured under unpolarised excitation conditions. Inset: UV-vis spectrum of Au nanorods dispersed in aqueous solution; b) calculated extinction, scattering and absorption spectra of a vertical 6×6 array with inter-nanorod distance of 1.2 nm. Inset: schematic of calculated array.

Ordered Au nanorod arrays possess distinctive optical properties and unique SERS effects owing to the large density of interparticle gaps. In particular, vertically aligned nanorod arrays were used for demonstration of SERS detection of biological species,[23] drug derivatives,[29] food contaminants[16,30] and molecular species.[25] The observed SERS high performances were explained by the high density of "hot spots", areas of extremely large field enhancements, generated in the superstructures. Finite-difference time domain method (FDTD) calculations have shown that hexagonally packed nanorods possess strong and uniform electromagnetic fields highly enhanced along the length of adjacent nanorods (see Figure S9), strongly decreasing with the increase of the inter-nanorod gap.[31] To demonstrate their SERS potential, we used nanorod arrays for detection of model molecule 4-ABT. Figure 6 shows the SERS spectrum of 4-ABT deposited in the gaps between assembled nanorods. The spectrum showed typical a_1 vibrational modes (in plane, in phase modes) at 1008, 1080, 1186, 1575 cm^{-1}. The spectrum also showed b_2 vibrational modes (out of plane, out of phase) at 1139, 1324, 1387 and 1435 cm^{-1}. The formation of b_2 peaks has been observed in SERS spectra of 4-ABT recorded on nanostructured surfaces and has been attributed to a metal-molecule charge transfer related to a chemical enhancement process.[32-35] In contrast the Raman spectrum of bulk 4-ABT showed only a_1 vibrational modes at 1005, 1086, 1492 and 1575 cm^{-1}. The co-deposition of 4-ABT did not affect the order of formed vertical arrays, as shown in the SEM images of S11.

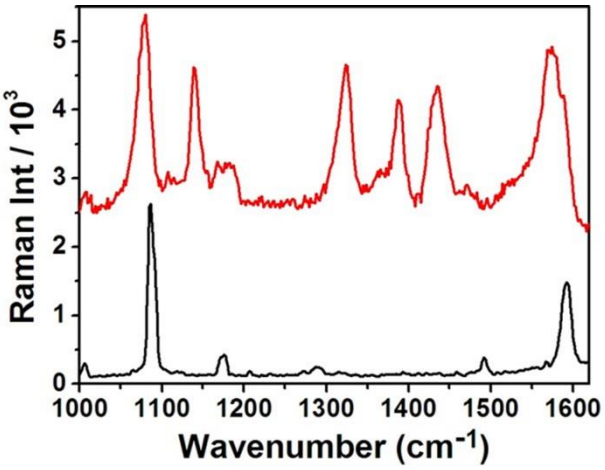

Figure 6. SERS spectrum of 4-ABT (red line); Raman spectrum of powder 4-ABT deposited on glass coverslip (black line).

Conclusions

In conclusion, droplet evaporation of organic solutions has been used for the facile fabrication of ordered vertical Au nanorod superstructures. The assembly process was fast, was controlled by the initial concentration of Au nanorod solutions and did not necessitate strict control on other experimental parameters such as temperature, surfactant concentration and substrate. Nanorod arrays displayed collective optical properties distinct from the optical properties of nanorod dispersed in solution. SERS detection of model molecule 4-ABT was shown in order to prove potential optical applications of fabricated arrays. The control of nanostructure order over large area shown in this paper constitutes an important development towards successful incorporation of superstructures into functional novel opto-electronic plasmonic devices. The understanding of mechanisms regulating the self-assembly process of nanorods into media different than water might extent potential applications of nanorods and their integration into functional hybrid devices.

ASSOCIATED CONTENT

Supporting Information Available: Synthesis of Au nanorods, influence of nanorod concentration, calculation of surface coverage, influence of nanorod aspect ratio, influence of evaporation rate, influence of the solvent, FDTD simulations of vertical arrays.

This material is available free of charge via the Internet at http://pubs.acs.org.

AUTHOR INFORMATION

Corresponding Author

* Daniela Iacopino, Tyndall National Institute, Dyke Parade, Cork, Ireland, e-mail: daniela.iacopino@tyndall.ie_.Phone: 00353(0)212346182.

Author Contributions

The manuscript was written through contributions of all authors. All authors have given approval to the final version of the manuscript. ‡These authors contributed equally. (match statement to author names with a symbol)

ACKNOWLEDGMENTS

This work was supported by the European Union Seventh Framework Programme (project 263091 Hysens and 265073 NANOWIRING)

REFERENCES

(1) Chen, H.; Lei, Q.; Wang J. Gold Nanorods and Their Plasmonic Properties. *Chem. Soc. Rev.* **2013**, 42, 2679-2724.

(2) Nie, Z.; Petukhova, A.; Kumacheva, E. Properties and Emerging Applications of Self-Assembled Structures Made from Inorganic Nanoparticles. *Nat. Nanotechnol*. **2010**, 5, 15 – 25.

(3) Zhang, S.-Y.; Regulatio, M. D.; Han, M.-Y.; Self-Assembly of Colloidal One-Dimensional Nanocrystals. *Chem. Soc. Rev*., **2014**, 43, 2301-2323.

(4) Lyvers, D.P.; Moon, J. A.; Kildishev, V.; Shalaev, V. M.; Wei, A. Gold Nanorod Arrays as Cavity Resonators. *ACS Nano* **2008**, 8, 2569-2576.

(5) Kullock, R.; Hendren, W. R.; Hille, A.; Grafström, S.; Evans, P. R.; Pollard, R. J.; Atkinson, R.; Eng, L. M. Polarization conversion through collective surface plasmons in metallic nanorod arrays. *Opt. Express* **2008**, 16, 21671-21681.

(6) G. A. Wurtz, R. Pollard, W. Hendren, G. P. Wiederrecht, D. J. Gosztola, V. A. Podolskiy, A. V. Zayats, Designed Ultrafast NonLinarity in a Plasmonic Nanorod Metamaterial Enhanced by Nonlocality. *Nat. Nanotechnol***. 2011**, 6, 107-111.

(7) Habouti, S.; Mátéfi-Tempfli, M.; Solterbeck, C.-H.; Es-Souni, M.; Mátéfi-Tempfli, S.; Es-Souni, M. On-Substrate, Self-standing Au Nanorod Arrays Showing Morphology Controlled Properties. *Nano Today* **2011**, 6, 12-19.

(8) Driskell, J. D.; Shanmukh, S.; Liu, Y.; Chaney, S. B.; Tang, X. –J.; Dluhy R. The Use of Aligned Silver Nanorod Arrays Prepared by Oblique Angle Deposition as Surface Enhanced Raman Scattering Substrates. *J. Phys. Chem. C* **2008**, *112*, 895-901.

(9) Hamon, C.; Postic, M.; Bizien, T.; Dupuis, C.; Even-Hernandez, P.; Courbin, L.; Gosse, C.; Atzner, F.; Marchi-Artzner, V. Three-Dimensional Self-Assembling of Gold Nanorods with Controlled Macroscopic Shape and Local Smectic B Order. *ACS Nano* **2012**, 6, 4137-4146.

(10) Thai, T.; Zheng, Y.; Ng, S. H.; Mudie, S.; Altissimo, M.; Bach, U. Self-Assembly of Vertically Aligned Gold Nanorod Arrays on Patterned Substrates. *Angew. Chem. Intern. Ed.* **2012**, 51, 8732-8735.

(11) Sigh, J. P.; Lanier, T. E.; Zhu, H.; Dennis, W. M.; Tripp, R. A.; Zhao, Y. Highly Sensitive and transparent Surface Enhanced Raman Scattering Substrate Made by Active Coldly Condensed Ag Nanorod Arrays. *J. Phys. Chem. C* **2012**, *116*, 20550-20557.

(12) Ming, T.; Kou, X.; Chen, H.; Wang, T.; Chen, H.-L.; Wang J. *Angew. Chem. Intern. Ed.* **2008**, 120, 9831-9836;

(13) Guerrero-Martínez, A. J. Pérez-Juste, E. Carbó-Argibay, G. Tardajos, L. M. Liz-Marzán, Gemini-Surfactant-Directed Self-Assembly of Monodisperse Gold Nanorods into Stadinf Superlattices. *Angew. Chem. Inter. Ed.* **2009**, 48, 9484-9488.

(14) Gómez- Graña, S.; Pérez-Just , J.; Alvarez-Puebla , R. A.; Guerrero-Martínez ,A.; Liz-Marzán, L. M. Self-Assembly of Au@Ag Nanorods Mediated by Gemini Surfactants for Highly Efficient SERS-Active Supercrystals. *Adv. Opt. Mater.* **2013**, 1, 477-481.

(15) Xie, Y.; Guo, S.; Ji, Y.; Guo, C.; Chen, Z.; Wu, X.; Liu Q. Self-Assembly of Gold Nanorods into Symmetric Superlattices Directed by OH-Terminated Hexa(ethylene glycol) Alkanethiol. *Langmuir* **2011**, 27, 11394-11400.

(16) Peng, B.; Li, G.; Dodson, S.; Zhang, Q.; Zhang, J.; Lee, Y. H.; Demir, H. V.; Ling, X. Y.; Xiong, Q. Vertically Aligned Gold Nanorod Monolayer on Arbitrary Substrates: Self-Assembly and Femtomolar Detection of Food Contaminants. *ACS Nano* **2013**, 7, 5993-6000.

(17) Xie, Y.; Guo, S.; Guo, C.; He, M.; Ji, Y. ; Chen, Z.; Wu, X.; Liu, Q. Xie, S. Controlable Two-Stage Droplet Evaporation Method and Its Nanoparticle Self-Assembly Mechanism. *Langmuir* **2013**, 29, 6232-6241.

(18) Mitamura, K.; Imae, T.; Saito, N.; Takai, O. Fabrication and Self-Assembly og Hydrophobic Gold Nanorods. *J. Phys.Chem. B* **2007**, 111, 891-8898.

(19) Alkilany, A. M.; Thompson L. B.; Murphy, C. J. Polyelectrolyte Coating Provides a Facile Route to Suspend Gold Nanorods in Polar Organic Solvents and Hydrophobic Polymers. *ACS Appl. Mater. Interfaces* **2010**, 2, 3417–3421.

(20) Schopf, C.; Martín. A.; Burke, M.; Quinn, A. J.; Iacopino, D. Au Nanorod Plasmonic Superstructures Obtained by a Combined Droplet Evaporation and Stamping Method. *J. Mater. Chem. C* **2014**, 2, 3536-3541.

(21) Martin, A.; Schopf, C.; Pescaglini, A.; O'Riordan, A.; Iacopino D. Synthesis, Optical Properties and Self-Assembly of Gold Nanorods. *J. Exp. Nanoscience* **2012**, 7, 688–702.

(22) Diefenbach, S.; N. Erhard, N.; Schopka, J.; Martin, A.; C. Karnetzky, C.; Iacopino, D.; W. Holleitner, A. Polarization Dependent, Surface Plasmon Induced Photoconductance in Gold Nanorod Arrays. *Phys. Stat. Sol.* **2014**, 8, 264-268.

(23) Alvarez-Puebla, R. A.; Agarwal, A.; Manna, P.; Khanal, B. P.; Aldeanueva-Potel, P.; Carbó-Argibaya, E.; Pazos-Pérez, N.; Vigderman, L.; Zubarev, E. R.; Kotov, N. A.; Liz-Marzán, L. M. Gold Nanorods 3D-Supercrystals as Surface Enhanced Raman Scattering Spectroscopy Substrates for the Rapid Detection of Scrambled Prions. *PNAS* **2011**, *108*, 8157-8161.

(24) Yang, J.; Wu, J-C.; Wang, J-K.; Chen, C-C.; Organic Solvent Dependence of Plasma Resonance of Gold Nanorods: A Simple Relationship. *Chem. Phys. Lett.* **2005**, *416*, 215-219.

(25) Martín, A; Pescaglini, A.; Schopf, C.; Scardaci, V.; Coull, R.; Byrne, L.; Iacopino, D. Surface-Enhanced Raman Scattering of 4-Aminobenzenethiol on Au Nanorod Ordered Arrays. *J. Phys. Chem. C* **2014**, 118, 13260-13267.

(26) Xiao, J.; Li, Z.; Ye, X.; Ma, Y.; Qi, L. Self-Assembly of Gold Nanorods into Vertically Aligned, Rectangular Microplates with Supercrystalline Structure. *Nanoscale* **2014**, 6, 996-1004.

(27) Sau, K. T.; Murphy, C. J. Self-assembly Patterns Formed Upon Solvent Evaporation of Aqueous Cetyltrimethylammonium Bromide-Coated Gold Nanoparticles of Various Shapes. *Langmuir* **2005**, *21*, 2923-2929.

(28) Nikoobakht, B.; Wang, Z. L.; El-Sayed, M. A. Self-Assembly of Gold Nanorods, *J. Phys. Chem. B* **2000**, *104*, 8635-8640.

(29) Sanles-Sobrido, M.; Rodriguez-Lorenzo, L.; Lorenzo-Abalde, S.; Gonzáles-Fernández, A.; Correa-Duarte, M. A.; Alvarez-Puebla, R. A.; Liz-Marzán, L. Label-Free SERS Detection of Relevant Bioanalytes on Silver-Coated Carbon Nanotubes: The Case of Cocaine. *Nanoscale* **2009**, *1*, 153-158.

(30) Martín, A.; Wang, J. J.; Iacopino, D. Flexible SERS Active Substrates for Ordered Vertical Au Nanorod Arrays. *RSC Adv.* 2014, *4*, 20038-20043.

(31) Doherty, M. D.; Murphy, A.; McPhillips, J.; Pollard, R. J.; Dawson, P. Wavelength Dependence of Raman Enhancement from Gold Nanorod Arrays: Quantitative Experiment

and Modelling of a Hot Spot Dominated System. *J. Phys. Chem. C* **2010**, 114, 19913-19919

(32) Osawa, M.; Matsuda, N.; Yoshii, K.; Uchida, I. Charge transfer Resonance Raman Process in Surface-Enhanced Raman Scattering from p-Aminothiophenol Adsorbed on Silver: Herzbeg-Teller Contribution. *J. Phys. Chem.* **1994**, *98*, 12702-12707.

(33) Lombardi, J. R.; Birke, R. L. A Unified Approach to Surface-Enhanced Raman Spectroscopy, *J. Phys. Chem. C* **2008**, *112*, 5605-5617.

(34) Hu, X.; Wang, T.; Wang, L.; Dong, S. Surface-Enhanced Raman Scattering of 4-Aminothiophenol Self-Assembled Monolayers in Sandwich Structure with Nanoparticle Shape Dependence: Off-Surface Plasmon Resonance Conditions. *J. Phys. Chem. C* **2007**, *111*, 6962-6969.

(35) Uetsuki, K.; Verma, P.; Yano, T.; Saito, Y.; Ichimura, T.; Kawata, S. Experimental Identification of Chemical Effects in Surface Enhanced Raman Scattering of 4-Aminothiophenol. *J. Phys. Chem. C*, **2010**, *114,* 7515-7520.

SYNOPSIS (Word Style "SN_Synopsis_TOC"). If you are submitting your paper to a journal that requires a synopsis, see the journal's Instructions for Authors for details.

TOC

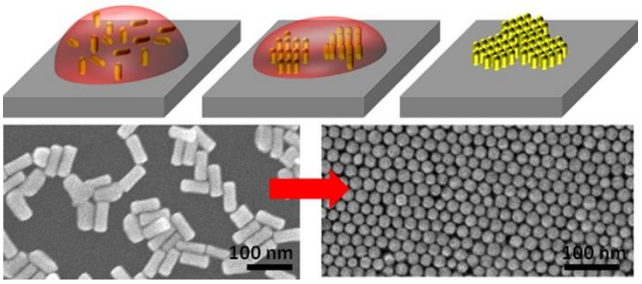

Formation of ordered vertical arrays by droplet deposition of Au nanorod organic solutions